Int. J. Electrochem. Sci., 10 **(2015)** 545 - 558

International Journal of
ELECTROCHEMICAL
SCIENCE
www.electrochemsci.org

Effects of Iron Bacteria on Cast Iron Pipe Corrosion and Water Quality in Water Distribution Systems

QI Beimeng[1,2,*], *Cui Chongwei*[1,2] *and Yuan Yixing*[1,2]

[1]State Key Laboratory of Urban Water Resource and Environment, Harbin Institute of Technology, HIT
[2]School of Municipal and Environmental Engineering, Harbin Institute of Technology, HIT, Harbin China, 150090.
[*]E-mail: qibeimeng@hotmail.com

Received: 6 August 2015 / *Accepted:* 19 October 2015 / *Published:* 1 December 2015

The corrosion behavior of cast iron influenced by bacteria was studied in the presence of iron bacteria, with sterile water acting as a reference. The corrosion process and corrosion scales were characterized by electrochemical and surface analysis methods. The results indicated that iron bacteria favored the formation of corrosion products due to the microbial activity, hence inhibiting the corrosion process periodically. With the breaking off of corrosion products and biofilms, corrosion, cast iron surfaces become more susceptible to corrosion and show higher corrosion rate. In the sterile water, no significant changes in E_{corr} were observed and the curve varied slightly whereas in the presence of iron bacteria, drastic changes of E_{corr} occurred between -0.745V and -0.658V. The values of R_{ct} under the abiotic condition were lower than those in the presence of iron bacteria due to the formation of a microcell with a small anode and a big cathode, indicating that iron bacteria play an important role in the corrosion process. Corrosion products formed with iron bacteria had a layered structure and heterogeneous distribution of floccules with different substances. Due to the metabolic activity, the growth and propagation of iron bacteria were closely related to the ferrous ion and dissolved oxygen concentration changes. Iron bacteria might lead to an increase of pH values and higher concentration of ferrous ion in bulk water.

Keywords: cast iron, iron bacteria, corrosion, water quality

1. INTRODUCTION

Cast iron pipes have been widely used in water distribution systems for centuries in several countries [1]. Cast iron has superior corrosion resistance in the atmosphere as witnessed by railway bridges that have existed for more than 100 years in the UK, USA and elsewhere in the world, but cast iron pipes are subjected to corrosion in the earlier stages of exposure, particularly in fresh water,

seawater and ground environments [2]. Internal corrosion in cast iron water pipes is the most common distribution system problem since corrosion is responsible for the decrease of transporting water capacity and the deterioration of potable water quality [3,4]. For example, the corroded systems may lead to an increase in Fe concentration, turbidity, quick decay of disinfectant residual and even suspensions of iron particles that give the tap water a yellow, brown color, or a dirty appearance [5].

Corrosion caused by microorganisms has been studied by many researchers, including iron bacteria, acidophilic Thiobacillus sp. and sulfate-reducing bacteria (SRB) [6]. It has been reported that the metabolic activity of microorganisms in corrosion scale played an important role in the biogeochemical redox cycling of iron oxidation [7, 8]. Many cases of corrosion damages were attributable to iron bacteria in chemical and water industries in the past few years. The majority of these cases were found in various carbon steel equipments including heat exchangers (i.e., tubes and connection pipelines), extinguisher pipelines and sections in water distribution systems [9]. Chamritski et al. [10] founded that iron bacteria can result in minor localized corrosion damage of stainless steel by under-deposit (i.e., crevice) corrosion. Several pitting attack was detected beneath the deposits, from which iron bacteria could be constantly isolated.

Iron bacteria that are also called metal-depositing microorganisms are commonly referred as causing microbiologically influenced corrosion (MIC) in many studies [11]. They are possible to metabolize reduced iron in their aqueous habitat, and then release it in the form of hydrate ferric oxide on or in their mucilaginous secretions [12, 13]. They can cause piping clogged with rusty sludge and unpleasant smell and taste. Besides, iron bacteria are capable of increasing the organic content in bulk water favoring the multiplication of other bacteria although they do not cause health problems in people directly. For example, the opportunities of sulfur bacteria infestation may be improved, and SRB probably grow quickly in the locally anaerobic environments provided by iron bacteria beneath the iron-rich tubercles [13, 14].

The mechanism of iron corrosion is related to electrochemical or/and microbial process. The reaction of iron pipes is considered to be a complicated process that is affected by bulk water quality including pH, temperature, oxygen concentration, alkalinity and the presence of sulfate and chlorine, etc. [15]. Iron bacteria have the capability of converting ferrous to ferric ions, that afterword precipitating as ferric hydroxide, and they can obtain energy from the redox process for growth [16]. It is reported that iron bacteria may produce large amounts of iron oxide precipitates during a very short time, and the iron oxidation rate under biotic condition can be ten to hundreds of times higher than that of abiotic condition [17].

Little and Wagner considered that the corrosion occurred in the presence of iron bacteria followed the crevice corrosion mechanism. The role of iron bacteria is to produce oxygen concentration areas and divide the metal surface into small anodic sites and large surrounding cathodic zone beneath biofilms and deposit layers [16, 18]. In addition, the deposit layers formed by iron bacteria could also create condensed oxygen zones and initiate crevice corrosion in water systems containing corrosion inhibitors. The corrosion rate beneath the rust deposits remains high because of the low penetrability of corrosion inhibitors and declining of local oxygen concentration where the site might turn anodic [19].

Despite a large number of research papers have been reported on the corrosion process of carbon steel, the quantitative data and information about the corrosion of cast iron pipes in water distribution systems is relatively scare. Also, previous researchers mainly focused on the study of corrosion behavior in the presence of SRB [16, 18, 20]. The real role of iron bacteria in cast iron corrosion is still not clear. It is difficult to state, due to lack of information and evidence, that the mechanism describing iron corrosion in water distribution systems. The necessary information is not adequate on the role of iron bacteria in corrosion initiation and propagation in the cathodic reaction occurring on iron surfaces which are covered by rust deposits. The present study is an attempt to simulate the corrosion process of cast iron in water contaminated with iron bacteria. The objective of this study was to investigate the effect of iron bacteria on the corrosion characteristics and electrochemical behavior of cast iron coupons in drinking water, with sterile water acting as a reference.

2. MATERIALS AND METHODS

2.1. Materials and preparation

The corrosion specimens were cut from cast iron water pipes (DN 1500), the nominal elemental composition (wt%) of cast iron coupons was: C 3.18, Si 2.37, S 1.08, Ca 0.26 and Fe balance. Square shape coupons with dimensions of 15mm×15mm× 5mm were selected in the experiment. An electrical contact was provided by a length of copper wire attached to the reverse side of each coupon mounted with an epoxy resin in order to create working electrodes. Prior to experiment, all coupons were sequentially abraded through a series of grit silicon carbide metallurgical paper (180 400 600 800) to a smooth surface. The polished coupons were degreased in acetone, followed by sterilizing in 75% ethanol for 6h, rinsed in sterile deionized water and dried in a desiccator. Each coupon was weighed after exposure of UV light before the experiment.

In the sterile experiment, ten cast iron coupons were immersed in sealed 2-L flasks containing 1.5L sterile water. For the biotic experiment implemented in parallel, the sterile water with the addition of iron bacteria solutions was used and the other ten coupons were exposed to iron bacteria. The two groups were both placed in incubators and kept in dark environment. Each coupon was taken out for measurements and analysis in corresponding experimental period.

2.2. Detection and culture of iron bacteria

The seed bacteria used in the study were isolated from rust deposits collected from the inner surface of iron pipes in water distribution systems during maintenance. They were incubated into the culture medium for enrichment at 30°C, and subsequently purified by picking up several single colonies using a sterile inoculation loop. The culture medium of iron bacteria consists of $(NH_4)_2SO_4$ 0.5g, $NaNO_3$ 0.5g, K_2HPO_4 0.5g, $MgSO_4 \cdot 7H_2O$ 0.5g, $CaCl_2 \cdot 6H_2O$ 0.5g, ammonium ferric citrate 10.0g, and distilled water 1000ml. The pH value was adjusted to 7.0 by appropriate amount of sodium

hydroxide before sterilizing at 121°C for 20 min. Iron bacteria were enumerated using Plate Counts method with Winogradsky's medium (g/L) [21]: 0.5 K_2HPO_4, 0.5 $NaNO_3$, 0.2 $CaCl_2$, 0.5 $MgSO_4 \cdot 7H_2O$, 0.5, NH_4NO_3 and 6.0 ammonium iron citrate (pH 6.8) under aerobic chamber.

2.3. Electrochemical measurement

Electrochemical measurements were conducted by 2273 electrochemical work station driven by POWERSUIT software package in a conventional three electrode cell, with a silver/silver chloride (Ag/AgCl 3M KCl) electrode as the reference electrode and a platinum grid as the counter electrode (Fig.1). The cell geometry was designed to expose a part of the coupon to the electrolyte with a surface area of 3.14cm^2, and the electrolyte selected in the research is 0.1M Na_2SO_4 aqueous solution.

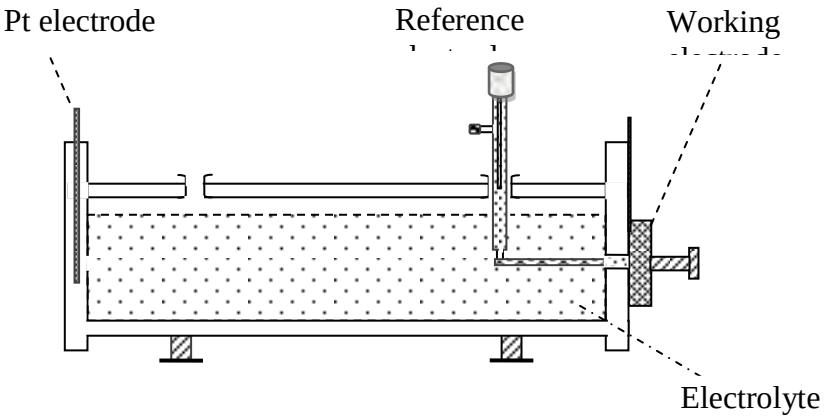

Figure 1. The three-electrode cell system

Polarization curves were obtained potentiodynamically and analyzed to determine corrosion potential (E_{corr}). The slowly scanning at a rate of 0.5mV/s was started at -1000mV below E_{corr} and terminated at 0mV versus the open circuit potential (OCP). Electrochemical impedance spectrum (EIS) measurements were performed at open circuit potential with a sinusoidal signal perturbation of 10mV over frequencies ranging from 10^5 to 10^{-2} Hz. The EIS results were analyzed by fitting the data to an equivalent circuit through Zsimpwin software.

Coupons were collected from the flasks with sterile water and iron bacteria solution at different times. Before potential scanning, a settling time of 10-15 min was required to make the open circuit potential stabilized. All electrochemical experiments were carried out at 26±2°C, and the results were obtained in triplicate for reproducibility to characterize corrosion behavior.

2.4. Surface analysis

The morphology and composition of corrosion scales were examined by scanning electron microscopy with elemental analysis (SEM-EDS Hitachi S-570) operating at 30kV on the surface of

cast iron coupons after 30–days exposure to media under biotic and abiotic conditions. The coupms were kept hydrated with the field water before preparation for microscopic examination. Prior to detection, the samples were dehydrated with acetone, then followed by coating with a thin gold film on the sample surface. Crystalline phase composition was analyzed using an X-ray powder diffractometer (XRD, Rigaku Corporation D/max-rB 12KW, Japan).

3. RESULTS AND DISSCUSION

3.1. Growth curve of iron bacteria

The growth curve of iron bacteria in the culture medium has been shown in Fig.2. The iron bacteria species isolated from rust deposits in cast iron pipes was defined as *A. baumannii,* a kind of Gram−negative, non-motile rod bacterium with high-affinity iron transport system (Fig.3) [22].

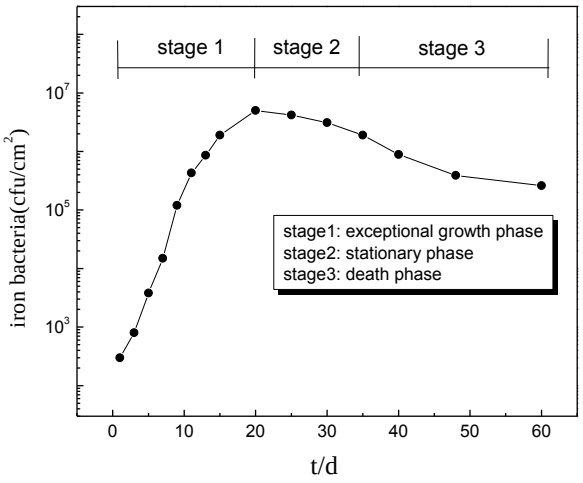

Figure 2. The growth curve of iron bacteria in the system

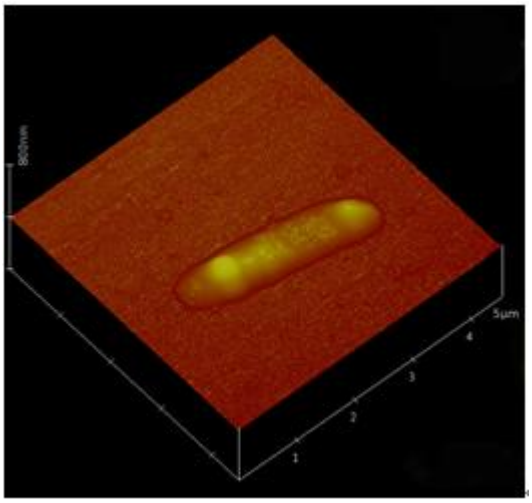

Figure 3. The appearance of iron bacteria by AFM

A typical three-stage growth cycle has been observed in the growth curve of iron bacteria. The first stage is an exceptional growth phase, where the amount of iron bacteria reaches a peak, 5.0×10^6 cfu/ml after 15days; the second stage is a stationary phase last for over 10days and the growth curve varies smoothly; the final stage is a death phase, the amount of iron bacteria declines indicating that a certain amount of iron bacteria disappeared.

3.2. Potential distributions

Fig.4 shows the variations of corrosion potential (E_{corr}) versus time of cast iron coupons after exposure to sterile water and iron bacteria. In the sterile water, no significant changes in E_{corr} were observed and the curve varied slightly, especially in the later stage. The gradual increase of E_{corr} began to stabilize after 20d. The electrode surface did not exhibit signs of visible corrosion after the termination of experiment, indicating that the cast iron coupons were in a passive state during the whole session. In the presence of iron bacteria, drastic increase of E_{corr} occurred from -0.745V to -0.658V in 10d then followed by an abrupt decline, and the curve reached a relatively steady phase after 30d. The potentials shift in the positive direction due to the formation of passive layer whereas the negative shift of E_{corr} can be attributed to either surface activation or dissolution of passive layer. Besides, the change of dissolved oxygen concentration can also lead to a decrease of cathode process rate, hence a shift of E_{corr} in the negative direction. The variation of E_{corr} with immersion time is consistent with the growth curve of iron bacteria, indicating the impact of iron bacteria on corrosion process of cast iron coupons.

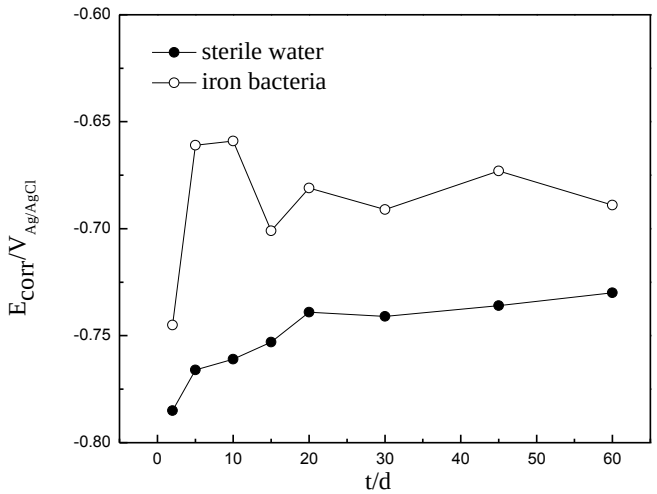

Figure 4. E_{corr} variations of cast iron coupons exposed to the sterile water and iron bacteria

Fig.5 illustrates that there are no essential differences in shapes of potentiodynamic polarization curves as immersion with or without iron bacteria, indicating that the study system with iron bacteria has little impact on mechanisms of cathode and anode process on cast iron coupons. However, it is shown that the anodic process improves significantly with the growth of iron bacteria. The shapes of

potentiodynamic polarization curve change slightly after 20d, at which time iron bacteria suspended growing and developed towards stationary phase.

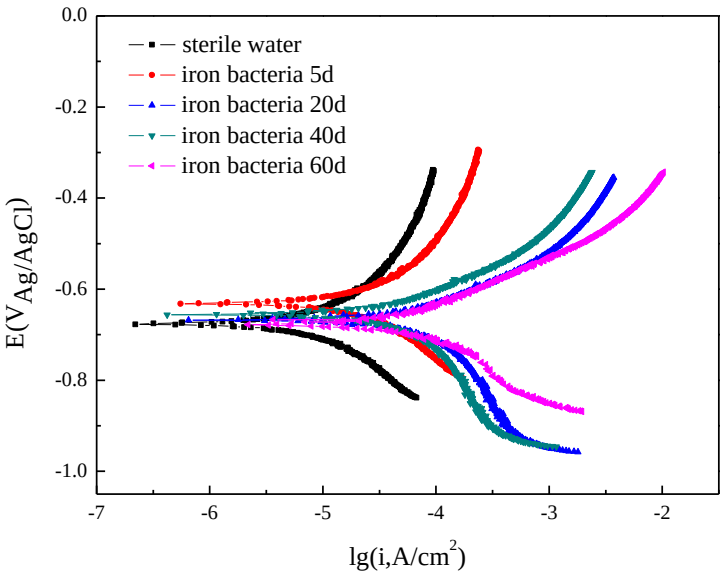

Figure 5. Potentiodynamic polarization curves of cast iron after exposure to the sterile water and iron bacteria

Based on the thermodynamics principle, the samples with lower corrosion potential tend to be corroded [23]. Therefore, the cast iron coupon exposed to sterile water is the most susceptible to corrosion. The polarization analyses indicate that the studied coupons become less susceptible to corrosion and show slower corrosion rate after exposure to iron bacteria due to the formation of passive layer. However, due to the instability of corrosion products, corrosion of cast iron may quickly propagate once the corrosion products break off. Pitting corrosion may also initiate on the surface since the corrosion products and biofilms are heterogeneous.

3.3. EIS analysis

Fig.6a shows the Nyquist plots of cast iron coupons after exposure to sterile water in different test times; it illustrates that the structure of EIS does not change significantly and the magnitudes of impedance increased with time. Compared to the impedance magnitudes obtained in the presence of iron bacteria (Fig.6b), the impedance magnitude in sterile water without iron bacteria was much lower. Fig.6b shows the Nyquist plots of cast iron samples immersed in sterile medium with iron bacteria during a growth cycle. The impedance magnitude variations developed with iron bacteria growth. It is found that the diameter of the semicircle representing the impedance increased significantly during the exceptional growth phase of iron bacteria and maintained stable in the stationary phase. The increase of impedance during exceptional growth phase is attributed to the formation of rust deposits and the mature of biofilms, for instance, the production of ferric hydroxide under aerobic condition that creates

a higher charge transfer resistance leading to the transient inhibition of the corrosion process [24]. The steady state of impedance may be related to the stabilization of biofilms and passive layers containing iron oxides or iron hydroxides on the surface of cast iron coupons. It is shown in Fig.6b that the impedance magnitude decreased after 30-days exposure to iron bacteria due to the changes of microenvironment.

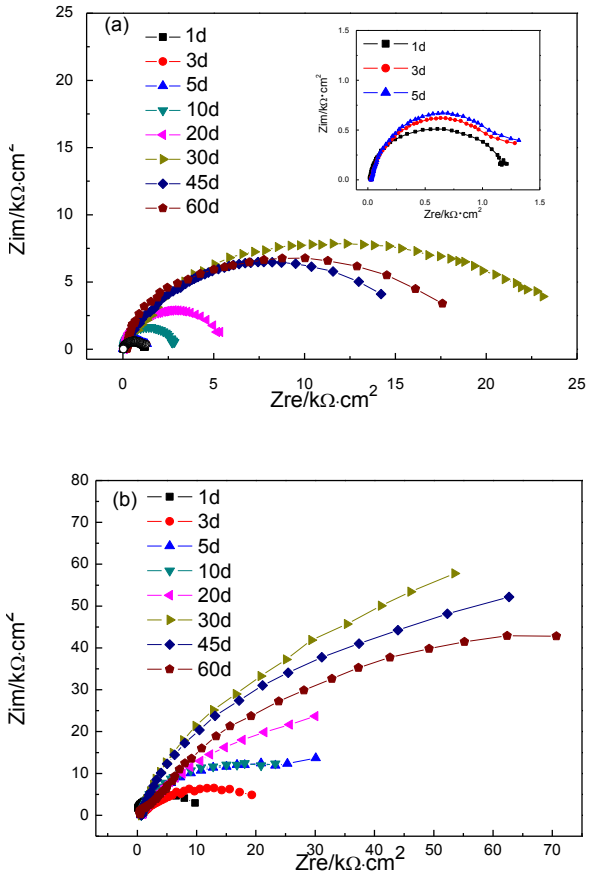

Figure 6. EIS of cast iron in sterile water (a) and iron bacteria (b) within different exposure time

To describe the impedance response of the corrosion behavior under different conditions, the EIS data was interpreted in the form of equivalent circuit with different time constants model as shown in Fig.7. For the iron bacteria free system, a two-time constant model fitting the EIS data is shown in Fig.7a, illustrating the existence of double layer and passive film under the abiotic condition. Fig.7b shows the equivalent circuit of the three-constant model fitting EIS results obtained in the presence of iron bacteria. The three constants are related to the double layer, the formation of biofilms and corrosion products. In corresponding circuits, R_s is the electrolyte resistance in bulk, R_{pf} and Q_{pf} repensent the resistance and capacity of passive layer respectively, R_{ct} and Q_{dl} represent the charge transfer resistance at the metal surface and capacity of the double layer, R_b and Q_b are the resistance and capacity of biofims.

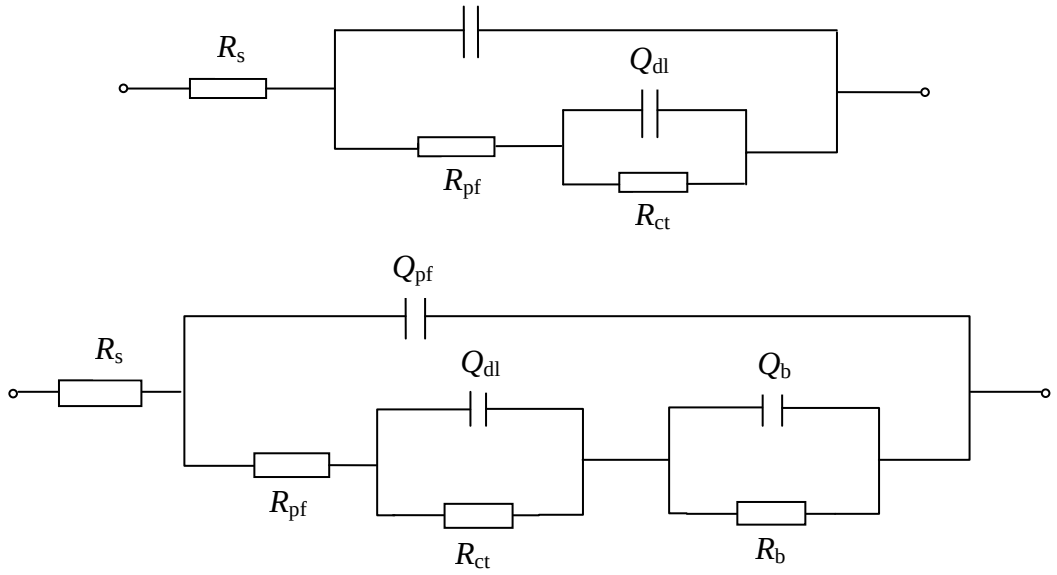

Figure 7. The fitting equivalent circuits of EIS for cast iron in the culture medium of iron bacteria (a) R_s (Q_{pf} [R_{pf} (Q_{dl} R_{ct})]) and (b) R_s (Q_{pf} [R_{pf} (Q_{dl} R_{ct}) (Q_b R_b)])

Fig.8 shows the time-dependant change of R_{ct} obtained from Nyquist plots. R_{ct} is considered to be a standard for evaluating the corrosion rate of metal. The values of R_{ct} fluctuated with immersion time, under the abiotic condition, R_{ct} were lower than those in the presence of iron bacteria due to the formation of a microcell with a small anode and a big cathode. In sterile water, R_{ct} increased gradually and tended toward 86.88 kΩ at 45d. In the presence of iron bacteria, R_{ct} exhibited a great increase from 26.75 kΩ to 162.25 kΩ at 30d, indicating the enhancement of corrosion inhibition with time, and then decreased to 106.07 kΩ at 60d.

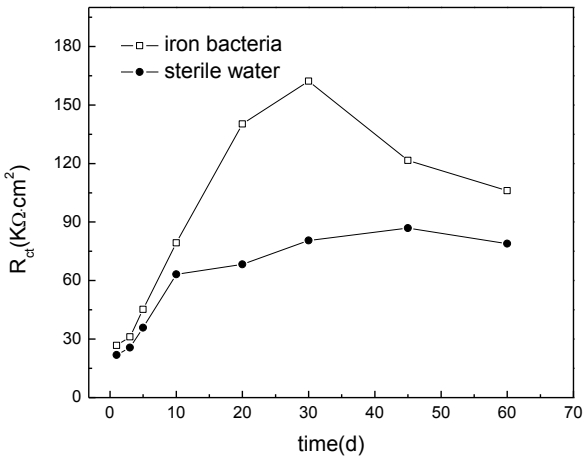

Figure 8. The variation in R_{ct} values that occurred in the sterile water and iron bacteria

With the decrease of biofilms and corrosion products adhesion, passive layers partially exfoliated and free metal surface acted as anode whereas corrosion products or biofilms acted as

cathode leading to the acceleration of iron corrosion. The interface reaction is mainly influenced by the resistance of the biofilm. The protective ability and activity of the biofilm decline with the decrease of iron bacteria. R_{ct} variations give the results essentially in agreement with the growth curve of iron bacteria as shown in Fig.2. The results are also in accordance with Sheng and González's works [25,26]. They have concluded that the morphology of biofilms has a great impact on corrosion, and a dense biofilm may in some instances act as a protective film on the metal surface.

The increase of R_{ct} derives from the increasing thickness of biofilms and passive layers. Iron oxides layer may slow the oxygen diffusion from bulk water to sample surface and alter the dynamics of corrosion reactions [27, 28]. Due to the heterogeneous structure of corrosion products, oxygen reduction occurs within corrosion products rather than on the surface, hence the corrosion rate at these locations is accelerated compared to clean surface. In addition, the microbial adhesion may be improved in the presence of iron oxides because of the increasing surface roughness [29], and as a consequence microorganisms colonize and make cast iron coupons precipitation enhanced. Therefore, iron bacteria can affect the corrosion of cast iron by either biofilms or iron compounds formed by their metabolic activities.

3.4. SEM and EDS analysis

SEM and EDS showed the morphology and chemical compositions of corrosion products formed on the surface of cast iron coupons immersed in sterile water and iron bacteria solutions after 60 days (Fig.9). The EDS results of corrosion products are listed in Table 1. It should be noted that the structure of corrosion products detected on the coupon surface within sterile water significantly differs from that immersed in the presence of iron bacteria. SEM revealed that the surface of cast iron coupon after exposure to sterile water covered with spongy brownie deposits. Spherical granules in which iron was the predominant species according to EDS analysis disorderly located in the upper layer of deposits [30]. The chlorine and manganese elements are not observed in corrosion products in sterile water.

Table 1. The EDS analysis of corrosion products formed on the surface

Element	Element content (atom%)			
	Without iron bacteria		With iron bacteria	
	1	2	1	2
Si	4.5730	5.0987	4.4033	4.9076
S	1.8137	1.1765	0.1748	0.1454
Cl	–	–	0.0918	0.0564
Ca	0.3528	0.4231	0.0850	0.1123
Mn	–	–	0.3111	0.1907
Fe	93.2605	94.1753	94.9340	93.1709

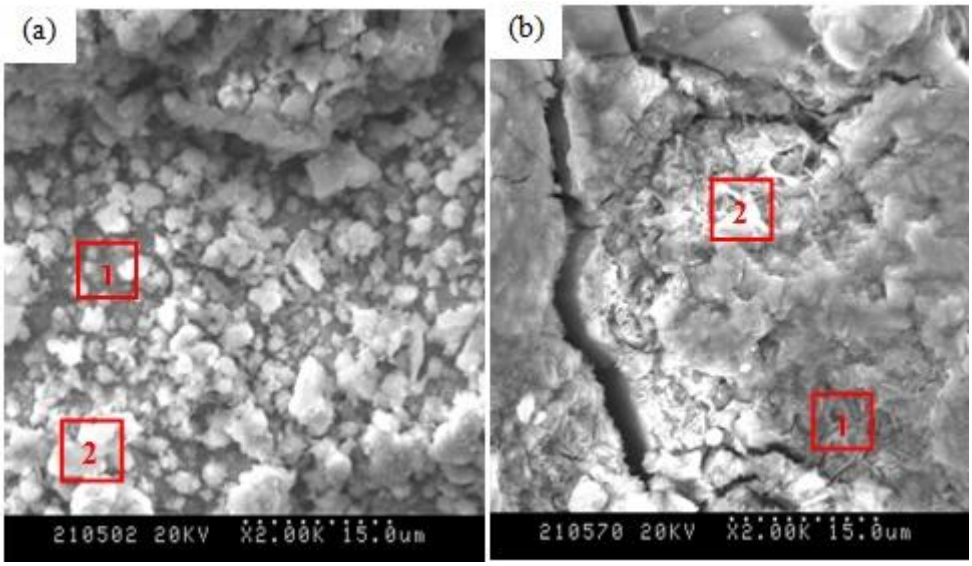

Figure 9. SEM micrographs of corrosion products on the sample surface (a) without iron bacteria and (b) with iron bacteria

Corrosion products formed with iron bacteria had a layered structure, which is in accordance with the EIS results, and a heterogeneous distribution of floccules (e.g. ferric oxide) with different substances. EDS analysis indicated a high concentration of iron (94.934 atom%) and a small amount of silicon, manganese and chlorine at 4.4033, 0.3111 and 0.0918 atom% respectively in the darker position 1. The higher concentration of sulfur (0.1748 atom%) in darker place is related to the formation of FeS. Small cracks were distributed irregularly beneath the upper layer and the corrosion product was composed of needle-like compounds. The initiation and propagation of pitting corrosion were related to cracks that may result in discontinuities of biofilms. The biofilms with a non-uniform structure contained iron bacteria, corrosion products, scales and other organic matters, and might favor the production of electrochemical cells causing the initiation of pitting [7,31].

3.5. Variations of the environmental parameters

The corrosion process caused by iron bacteria is related to pH, the concentration of ferrous ion and dissolved oxygen (DO) in bulk water. Fig.10 shows the changes that occurred in pH values within sterile water iron bacteria. In sterile water, pH ranged from 6.99 to 7.05 whereas in the presence of iron bacteria it reached a peak value of 7.10 at 60 d. Although the changes in pH values exhibited irregular orientations, pH values were higher with iron bacteria growth compared to sterile water. The discrepancy of pH values under biotic and abiotic conditions may be attributed to the difference in the accumulation of organic acids based on the amount variation of active iron bacteria. In addition, the variation of pH is related to crystalline compounds of corrosion products. It has been reported that ferrihydrite was found abundantly in rust deposits. Ferrihydrite possibly convert to lepidocrocite in neutral environment in short time and pH may increase with the accumulation of.

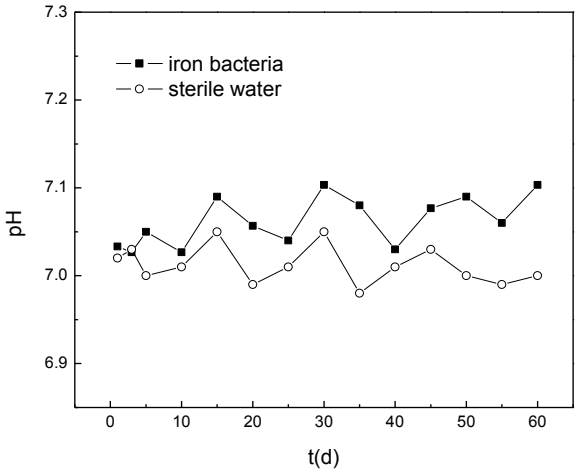

Figure 10. The changes of pH value in the sterile water and iron bacteria solutions

Fig.11 shows the ferrous ion concentration in sterile water and iron bacteria at different times. In sterile water, the ferrous ion concentration ranged from 0.30 mg/L to 0.46mg/L and maintained at a relatively stable state although there were fluctuations during the whole experiment time. Due to the metabolic activity, the growth and propagation of iron bacteria were closely related to ferrous ion concentration changes. Hence in the presence of iron bacteria, the ferrous ion concentration varied with the growth of iron bacteria. In the exceptional growth phase of iron bacteria, ferrous ion concentration quickly decreased to 0.39 mg/L at 20 d since iron bacteria generated energy by oxidation ferrous to ferric ions, and remained stable in the following 10 days. The formation of stable corrosion products (e.g. ferroferric oxide) may impede the iron release in the later stage. The increase of ferrous ion concentration after 30 d could be attributed to the decreasing amount of iron bacteria. Moreover, the corrosion products including goethite, lepidocrocite and ferrous carbonate formed on the surface were unstable and easy to fall off. For example, ferrous carbonate is favorable to release iron ions into the bulk water [32], thus increasing ferrous ion concentration. Corrosion products formed on the surfaces of cast iron coupons in sterile water were more protective against corrosion than those in the medium of iron bacteria, which was in agreement with the lower iron release in sterile water.

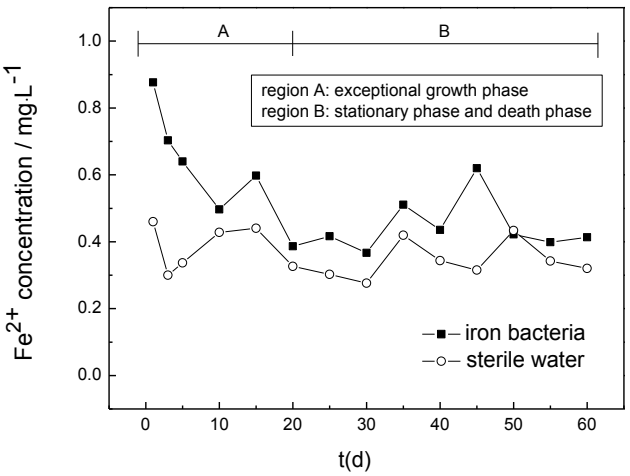

Figure 11. The variation of ferrous ion in the sterile water and iron bacteria solutions

DO concentration measured throughout exposure for different immersion tests is shown in Fig.12. Cast iron coupons exposed to iron bacteria showed a sharp decrease of DO concentration with time in the exceptional growth phase of iron bacteria during the first 20 days. This oxygen depletion could be attributable to the microbial activity of bacteria. Afterwards, DO levels remained fairly steady until the completion of the exposure whereas in sterile water, DO changes showed a slow decline with time throughout the whole experiment, indicating that the growing process of iron bacteria can induce changes of dissolved oxygen in bulk water.

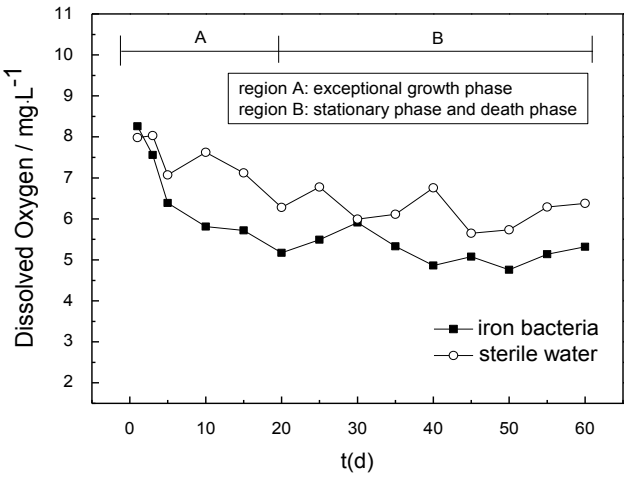

Figure 12. The changes of dissolved oxygen in the sterile water and iron bacteria solutions

4. CONCLUSION

The results indicated that corrosion was more rapidly inhibited on cast iron coupons in the presence of iron bacteria than those in the sterile water due to the formation of passive layer in the early stage. With the decrease of passive layer adhesion, the corrosion process was accelerated and iron release became higher. The variation of E_{corr} with immersion time was consistent with the growth curve of iron bacteria. EIS results showed that R_{ct} under the abiotic condition were lower than those in the presence of iron bacteria due to the formation of a microcell with a small anode and a big cathode indicating that passive layers were formed more slowly.

Corrosion products formed with iron bacteria had a layered structure and a heterogeneous distribution of floccules with different substances. There were no clear pitting holes observed by SEM, and small cracks were distributed irregularly beneath the upper layer. In sterile water, the slow formation of corrosion products may be more homogeneous and favored the production of dense and compact passive layers which could increase the corrosive resistance. Iron bacteria could also induce changes of the environment. The pH values were higher with iron bacteria growth compared to sterile water and due to the metabolic activity, the iron release was higher and DO concentration decreased more rapidly.

ACKNOWLEDGEMENTS
This work was supported by National Natural Science Foundation of China (Grant No.51178141). The authors would like to thank for the financial support.

References

1. H. B. Wang, C. Hu, X. X. Hu, M. Yang, J. H. Qu, *Water Res.*, 46 (2012) 1070.
2. Robert E. Melchers, *Corros. Sci.*,68 (2013) 186.
3. T. L. Gerke, J. B. Maynard, M. R. Schock, D. L. Lytle, *Corros. Sci.*, 50 (2008) 2030.
4. L. L. Machuca, L. Murray, R. Gubner, S. I. Bailey, *Mater. Corros.*, 65 (2014) 8.
5. C. Y. Peng, G. V. Korshin, R. L. alentine, A. S. Hill, M. J. Friedman, S. H. Reiber, *Water Res.*,44 (2010) 4570.
6. K. A. Zarasvand, V. R. Rai, *Int. Biodeterior. Biodegrad.*, 87 (2014) 66.
7. B. Qi, B. Wang, C. Wu, Y. Yuan, *Int. J. Electrochem. Sci.*, 10 (2015) 1813.
8. D. A. Lytle, T. L. Gerke, J. B. Maynard, *J. Am. Water Works Assoc.*, 97 (2005) 572.
9. J. O. Starosvetsky, R. Armon, A. Groysman, D. Starosvetsky, *Mater. Perform.*, 38 (1999) 55.
10. I. G. Chamritski, G. R. Burns, B. J. Webster, *Corros.*, 60 (2004) 658.
11. N. Muthukumar, S. Mohanan, S. Maruthamuthu, P. Subramanian, N. Palaniswamy, M. Raghavan, *Electrochem. Commun.*, 5 (2003) 421.
12. Liz Karen Herrera, Hector A. Videla, *Int. Biodeter. Biodegr.*, 63 (2009) 891.
13. C. Xu, Y. Zhang, G. Cheng, W. Zhu, *Mater. Sci. Eng.*, 443 (2007) 235.
14. Barham Hamah-Ali, Brahim Si Ali, Rozita Yusoff, Mohamed Kheirodin Aroua, *Int. J. Electrochem. Sci.*, 6 (2011) 181.
15. Jacek Nawrocki, Urszula Raczyk-Stanis1awiak, Joanna S´ wietlik, Anna Olejnik, Miros1awa J. Sroka, *Water Res.*, 44 (2010) 1863.
16. Y. C. Chen, C. M. Lee, S. K. Yen, S. D. Chyou, *Corros. Sci.*, 49 (2007) 3917.
17. D. Starosvetsky, R.Armon, J. Yahalom, J. Starosvetsky, *Int. Biodeter. Biodegr.*, 47 (2001) 79.
18. B. Little, P. Wagner, *Mater. Perform.*, 36 (1997) 40.
19. F. Teng, Y. T. Guan, W. P. Zhu, *Corros. Sci.*, 50 (2008) 2816.
20. T. S. Rao, T. N. Sairam, B. Viswanathan, K. V. K. Nair, *Corros. Sci.*, 42(2000) 1417.
21. R. M. Atlas, *Handbook of Microbiological Media*, CRC Press, Boca Raton, FL (1993).
22. C. W. Dorsey, M. S. Beglin, L. A. Actis, *J. Clin. Microbiol.*, 9 (2003) 4188.
23. F. Mansfeld, *Corros. Sci.*, 47 (2005) 3178.
24. F. Kuang, J. Wang, L. Yan, D. Zhang, *Electrochim. Acta.*, 52 (2007) 6084.
25. X. X. Sheng, Y. P. Ting, S. O. Pehkonen, *Corros. Sci.*, 49 (2007) 2159.
26. J. E. G. Gonzalez, F. J. H. Santana, J. C. Mirzarosca, *Corros. Sci.*, 40 (1998) 2141.
27. M. Sancy, Y. Gourbeyre, E. M. M.Sutter, B. Tribollet, *Corros. Sci.*, 52 (2010) 1222.
28. B. W. A.Sherar, P. G. Keech, D. W. Shoesmith, *Corros. Sci.*, 66 (2013) 256.
29. H. Wang, L. K. Ju, H. Castaneda, G. Cheng, B. Z. Newby, *Corros. Sci.*, 89 (2014) 250.
30. Y. Wan, D. Zhang, H. Liu, Y. Li, B. Hou, *Electrochim. Acta.*, 55 (2010) 1528.
31. J. Starosvetsky, D. Starosvetsky, B. Pokroy, T. Hilel b, R. Armon, *Corros. Sci.*, 50 (2008) 540.
32. Z. J. Tang, S. K. Hong, W. Z. Xiao, J. Taylor, *Corros. Sci.*, 48 (2006) 322.